

# Influence of Impact Parameter Fluctuations on Transverse Momentum Fluctuations

**Katarzyna Grebieszko**

Warsaw University of Technology

e-mail: kperl@if.pw.edu.pl

## Abstract

The preliminary NA49 results on the energy dependence of transverse momentum fluctuations over the whole Super Proton Synchrotron (SPS) energy range exhibit an unexpected effect. The  $\Phi_{p_T}$  fluctuation measure - used by the NA49 experiment - manifests a different behavior for different charge combinations. Whereas the  $\Phi_{p_T}$  is consistent with zero and independent of energy for negatively charged particles, it significantly increases for both all charged and positively charged particles at lower SPS energies. The string-hadronic ultrarelativistic quantum molecular dynamics model (UrQMD) is applied here to explain this effect. The UrQMD simulations show that the number of protons is strongly correlated with impact parameter and that the event-by-event impact parameter fluctuations are responsible for the event-by-event transverse momentum fluctuations of positively charged and all charged particles where protons are included. The observations presented in this article are important for all experiments measuring event-by-event fluctuations, especially for those using all charged particles in the analysis. The results can be also crucial for detectors with acceptances extending to the beam/target spectator domains.

# 1 Introduction

Event-by-event fluctuations of kinematic characteristics and particle yields are believed to be one of the important probes to study the dynamics of heavy-ion collisions. Transverse momentum and multiplicity fluctuations are expected to be modified when the system approaches the phase boundary between hadron gas and quark-gluon plasma (QGP). It has been also argued that significant transverse momentum and multiplicity fluctuations should appear for systems hadronizing near the second-order critical QCD end-point [1]. The QCD phase diagram -  $(T, \mu_B)$ , where  $T$  is the temperature and  $\mu_B$  bariochemical potential - can be scanned both by varying the system size/centrality and energy and therefore a possible nonmonotonic evolution of event-by-event ( $p_T$  and multiplicity) fluctuations with beam energy, system size, or centrality may be used as an indication of the phase transition and the QCD critical point [1].

The NA49 experiment at the CERN SPS studied both the system size dependence and the energy dependence of transverse momentum fluctuations. In the analysis of the NA49 data the  $\Phi_{p_T}$  fluctuation measure - proposed in [2] - was used to quantify transverse momentum fluctuations on event-by-event basis (the definition and some properties of the  $\Phi_{p_T}$  measure are presented in the next section and in [2, 3]). The NA49 results exhibit a significant nonmonotonic structure of transverse momentum fluctuations with the system size at the top SPS energy [3]. Qualitatively the same structure was found for all possible charge selections i.e. for all charged, negatively charged, and positively charged particles.

However, the preliminary NA49 results on the energy dependence of transverse momentum fluctuations over the whole SPS energy range manifests an unexpected effect: the  $\Phi_{p_T}$  measure shows a different behavior for different charge selections (see [4] and Fig. 1). The  $\Phi_{p_T}$  is independent of energy and it is consistent with zero for negatively charged particles, but it significantly increases for lower SPS energies for both all charged and positively charged particles.

In this work it will be shown that the effect observed by the NA49 experiment is connected with protons only, and it can be explained by event-by-event impact parameter fluctuations or - more precisely - by a correlation between the number of protons in the forward hemisphere and the number of protons that are closer to the production region. The final conclusions from this analysis are important for all experiments measuring event-by-event fluctuations, especially for those that are using all charged particles in the analysis. It is also important for detectors with acceptances extending to the beam/target spectator domain. Due to a specific choice of the rapidity region (midrapidity only) the Relativistic Heavy Ion Collider (RHIC) experiments appear to be rather insensitive to the effects of impact parameter fluctuations - even if the analysis is performed by use of all charged particles registered in the detectors.

The analysis presented in this article is based on preliminary NA49 results [4] and on events generated within the UrQMD approach [5, 6, 7].

## 2 $\Phi_{p_T}$ fluctuation measure

Following the authors of [2] one defines a single-particle variable  $z_{p_T} = p_T - \overline{p_T}$  with the overbar denoting averaging over a single-particle inclusive distribution. Further, one introduces the event variable  $Z_{p_T}$ , which is a multiparticle analog of  $z_{p_T}$ , defined as

$$Z_{p_T} = \sum_{i=1}^N (p_{Ti} - \overline{p_T}), \quad (1)$$

where the summation runs over particles in a given event. Note, that  $\langle Z_{p_T} \rangle = 0$ , where  $\langle \dots \rangle$  represents averaging over events. Finally, the  $\Phi_{p_T}$  measure is defined as

$$\Phi_{p_T} = \sqrt{\frac{\langle Z_{p_T}^2 \rangle}{\langle N \rangle}} - \sqrt{z_{p_T}^2}, \quad (2)$$

where  $N$  is the average multiplicity of the considered particles. There are two most important properties of the  $\Phi_{p_T}$  measure. If the system consists of particles that are emitted independently from each other (no interparticle correlations)  $\Phi_{p_T}$  equals zero. On the other hand, if A+A is an incoherent superposition of many independent N+N interactions (superposition model), then  $\Phi_{p_T}$  is independent of centrality and it has the same value for A+A and N+N collisions.

Several effects may lead to nonzero value of  $\Phi_{p_T}$ . Among them are those that occur on an event-by-event basis (event-by-event fluctuations of the inverse slope parameter, existence of different event classes, i.e., “plasma” and “normal” events), but there are also interparticle correlations due to Bose-Einstein statistics, Coulomb effects, resonance decays, flow, jet production, etc.

### 3 NA49 data

To study the energy dependence of transverse momentum fluctuations the NA49 experiment used samples of central Pb+Pb collisions at 20A, 30A, 40A, 80A and 158A GeV energy, corresponding to  $\sqrt{s_{NN}} = 6.27, 7.62, 8.73, 12.3$ , and 17.3 GeV, respectively. The fraction of the total inelastic cross section of nucleus+nucleus collisions ( $\sigma/\sigma_{tot}$ ) was set as equal to 7.2%. In the analysis only tracks with  $0.005 < p_T < 1.5$  GeV/c were used. For all five SPS energies the forward-rapidity region was selected as  $1.1 < y_\pi^* < 2.6$ , where  $y_\pi^*$  is the particle rapidity calculated in the center-of-mass reference system (particles were not identified in this analysis and their rapidities were calculated assuming the pion mass for all particles). Within the studied rapidity range the azimuthal angle acceptance of the NA49 detector -  $(p_T, \phi)$  - is not uniform and it is described by the analytical curves given in [4]. Additionally, it was demonstrated [4] that at lower SPS energies, the NA49 TPC acceptance extends to the projectile spectator domain and therefore the sample of particles can be contaminated by beam particles. For energies above 80A GeV the beam region and the region of particles - accepted by the NA49 for  $p_T$  fluctuations analysis - do not overlap.

The preliminary NA49 results on the energy dependence of transverse momentum fluctuations are presented in Fig. 1 (points). Separate panels correspond to all charged particles, negatively charged and positively charged particles used in the analysis. A significant decrease of transverse momentum fluctuations with increasing energy is observed for positively charged particles, whereas for the negatively charged ones  $\Phi_{p_T}$  values are independent of energy.

### 4 UrQMD predictions

The  $\Phi_{p_T}$  values measured by the NA49 experiment are compared to the predictions of the UrQMD model [5, 6, 7]. The UrQMD generator is a microscopic transport model producing hadrons via formation, decay, and rescattering of resonances and strings. The UrQMD approach simulates multiple interactions of both target/beam nucleons and newly

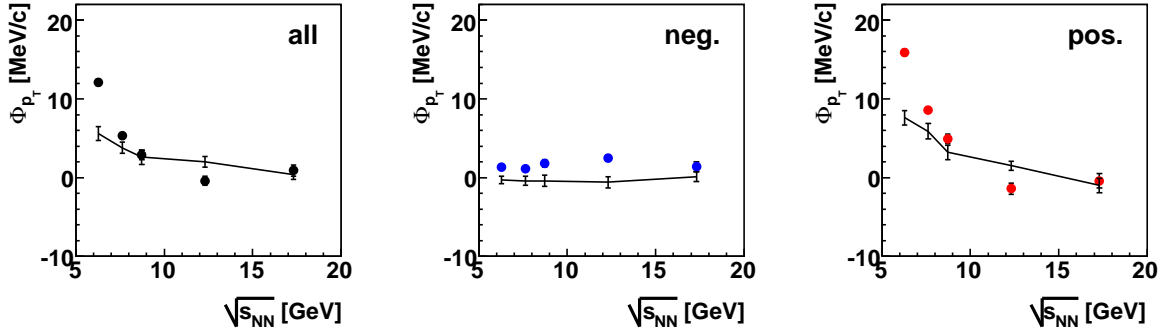


Figure 1: (Color online)  $\Phi_{p_T}$  as a function of energy calculated from the UrQMD model (lines) with the acceptance restrictions the same as for the preliminary NA49 data [4]. UrQMD calculations are compared to preliminary NA49 data (points) taken from [4]. The panels represent: all charged, negatively charged, and positively charged particles, respectively.

produced particles, excitation, and fragmentation of color strings and the formation and decay of hadronic resonances. In this analysis default parameters of the model have been used (meson-meson and meson-baryon scattering included). For each energy, from the sample of minimum bias Pb+Pb events, the most central 7.2% interactions have been selected, similarly as in the real NA49 events. Such selection corresponds to the impact parameter range  $0 < b < 4.35$  fm (in the generated histogram of impact parameter values the number of entries  $N(b)$  was set as proportional to  $const \cdot b$  [fm]).

The NA49 experiment used all charged particles, originating from the main vertex, to determine the  $\Phi_{p_T}$  measure. It means practically that only main vertex pions, protons, and kaons and their antiparticles were used in the analysis, because particles coming from the decays of  $\Lambda$ ,  $\phi$ ,  $\Xi$  and  $\Omega$  are believed to be rejected by a set of track selection criteria. Therefore the analysis of the UrQMD events has been carried out also by use of all charged pions, protons, and kaons and their antiparticles. In the analysis of the UrQMD events the same kinematic and acceptance restrictions have been applied as in the case of the NA49 data. In principle, the selected  $p_T$  - azimuthal angle acceptance ( $p_T, \phi$ ) is common for all five SPS energies and it corresponds to the restrictions used in the NA49 analysis (for details see [4]).

Fig. 1 presents the comparison of the  $\Phi_{p_T}$  versus energy for the preliminary NA49 data (points) and for the UrQMD model (lines). Both the preliminary NA49 data and the UrQMD model show qualitatively the same behavior. The UrQMD model confirms a significant decrease of transverse momentum fluctuations with increasing energy for positively charged particles. On the other hand, there is no energy dependence of  $\Phi_{p_T}$  for negatively charged particles. In the previous article of the NA49 [3] the system size dependence of transverse momentum fluctuations was studied and a nonmonotonic structure of  $\Phi_{p_T}$  appeared, but the shape of this dependence was very similar for all three charge selections. Therefore, the fact that the energy dependence of  $\Phi_{p_T}$  is qualitatively different for various charge selections seems to be quite surprising. As the  $\Phi_{p_T}$  value for all charged particles can be treated as a nontrivial combination of  $\Phi_{p_T}$  for negatively and positively charged particles (additional sources of fluctuations, however, are not excluded), a main emphasis should be placed on understanding the qualitative difference between positively and negatively charged particles.

It should be also stressed that, - although the same kinematic and acceptance restrictions are used for the preliminary NA49 data and for the UrQMD events, - the  $\Phi_{p_T}$

values should not be directly compared in these two cases. One of the reasons is a fact that the UrQMD model does not include effects of short-range correlations (Bose-Einstein and Coulomb). Moreover, it has been already shown by the CERES experiment that the measured values of mean  $p_T$  fluctuations, calculated by use of the UrQMD model with default parameters, can be underestimated [8] and that switching off secondary scattering (in particular meson-baryon rescattering) results in the values of  $p_T$  fluctuations similar to those observed in the data. It has been also checked that this underestimation (when rescattering processes are included in the UrQMD model) can be even stronger for lower energies. The above effect, observed by the CERES experiment, might help in a qualitative explanation of the underestimation of the UrQMD  $\Phi_{p_T}$  values in Fig. 1.

## 5 Results for identified particles

The similar structure of the energy dependence of the  $\Phi_{p_T}$  measure for the NA49 data and for the UrQMD model encourages us to search for an explanation of the origin of the increased  $\Phi_{p_T}$  values for positively charged particles at lower SPS energies by analyzing effects incorporated in the model simulations. Although the track-by-track identification is not always possible in the data it is instructive to check - by use of the UrQMD model - what is the particle content in the studied forward-rapidity region. The NA49 sample of negatively charged particles is composed mainly of negative pions (94.4% of all negatives for 20A GeV and 89.4% of all negatives for 158A GeV) and negatively charged kaons (5.6% for 20A GeV and 9.2% for 158A GeV), whereas the number of antiprotons can be treated as negligible (below 0.1% for 20A GeV and 1.6% for 158A GeV). The sample of positively charged particles is less homogeneous, as it contains positive pions (42.8% for 20A GeV and up to 69% for 158A GeV), positive kaons (from 8.5% for 20A GeV to 10.4% for 158A GeV) and protons (48.7% for 20A GeV and 20.6% for 158A GeV). Within the NA49 kinematic and acceptance region the total multiplicity of the final state protons remains nearly constant for all five energies (11.1 - 13.2), in contrary to the multiplicities of newly produced (generated) particles such as  $\pi^+$  or  $K^+$ . Therefore, the fraction of protons in a sample of positively charged particles is significantly higher for lower energies and thus one can expect that the increased  $\Phi_{p_T}$  values for lower energies might be indeed due to protons. The qualitative verification of this hypothesis is presented in Fig. 2 where the  $\Phi_{p_T}$  values are presented separately for different types of final state particles. The right panel of Fig. 2 shows that the  $\Phi_{p_T}$  values for protons only (solid, thick curve) are very close to those for all positively charged particles (solid, thin curve) thus confirming that protons indeed are responsible for the increased  $\Phi_{p_T}$  values at lower energies. The  $\Phi_{p_T}$  measure obtained for newly produced particles such as pions, kaons (positively and negatively charged) or antiprotons is consistent with zero for all energies (in agreement with the hypothesis of weak interparticle correlations).

Although the precise track-by-track identification in the NA49 experiment is much less reliable than the statistical one, the similar analysis with identified particles was prepared also for the NA49 data. In order to identify particles the combined information on the ionization energy loss ( $dE/dx$ ) and total momentum (Bethe-Bloch curves) was used. The energy dependence of  $\Phi_{p_T}$  measure was calculated separately for charged pions and protons. Fig. 3 shows that the obtained NA49 results are in qualitative agreement with those from the UrQMD model, namely  $\Phi_{p_T}$  for pions (all charged and negatively and positively charged separately: solid curves) and for antiprotons (dashed curve in the middle panel) are consistent with zero, whereas  $\Phi_{p_T}$  versus energy for protons only

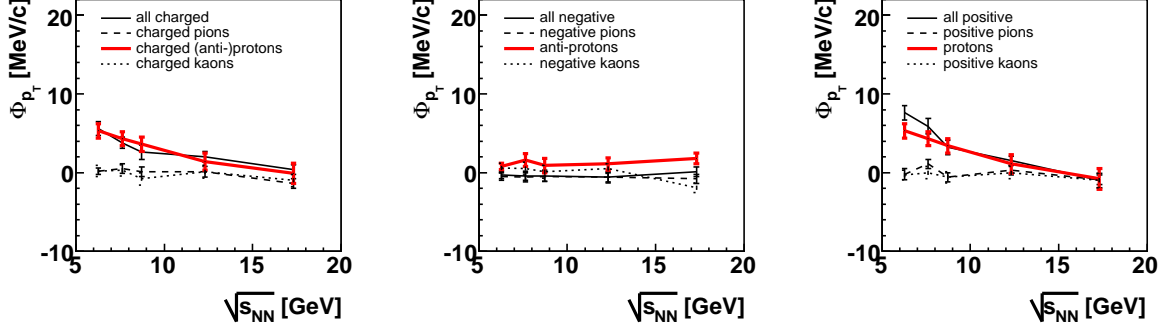


Figure 2: (Color online)  $\Phi_{p_T}$  versus energy calculated from the UrQMD model, separately for different types of produced particles. The kinematic cuts and acceptance restrictions for the UrQMD model are the same as for the preliminary NA49 data. Pion mass has been assumed for all produced particles.

(dashed curve in the right panel) follows a structure observed for protons in the UrQMD model (strong decrease with energy). The quantitative comparison of  $\Phi_{p_T}$  values - for positively charged particles and for protons only - is rather difficult because Bethe-Bloch identification leads to random losses of particles. The latter was found [3] to reduce strongly the magnitude of correlations. Also an additional cut on total momentum ( $p \geq 3$  GeV/c), applied to eliminate the region of intersection of Bethe-Bloch curves, reduces the magnitude of  $\Phi_{p_T}$  values.

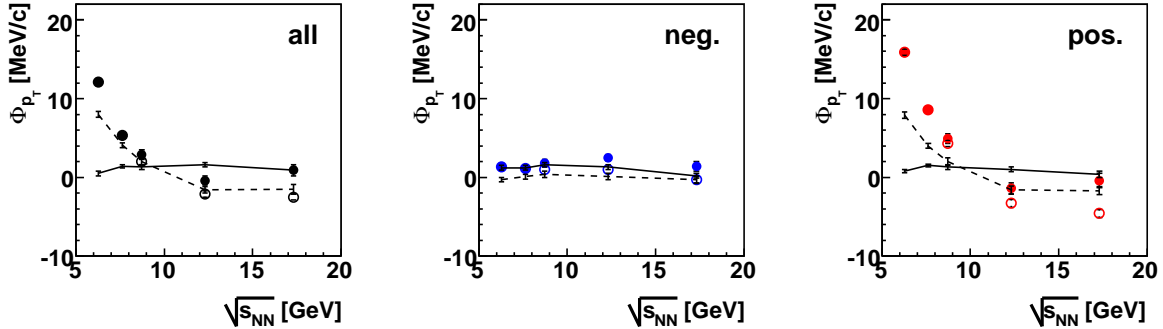


Figure 3: (Color online) The preliminary NA49 data on  $\Phi_{p_T}$  as a function of energy calculated for unidentified particles without two-track resolution corrections (open points) and with two-track resolution corrections (full points) compared to identified pions (solid curves) and (anti-)protons (dashed curves). Data for identified particles do not include two-track resolution corrections. For data with identification additional cuts on  $dE/dx$  values and total momentum ( $p \geq 3$  GeV/c) were applied. The panels represent: all charged, negatively charged, positively charged particles, respectively. Figure taken from [4].

## 6 Effect of the limited acceptance

It has been already stressed in many articles, that a *limited* acceptance can influence the observed values of fluctuation measures. (The NA49 experiment measured  $p_T$  fluctuations with a specific choice of azimuthal angle -  $(p_T, \phi)$  curves defined in [4].) Therefore, as the next step, it should be verified whether the energy dependence of  $\Phi_{p_T}$  exhibits qualitatively

the same structure when using complete azimuthal angle acceptance. The dashed lines in Fig. 4 represent the energy dependence of  $\Phi_{p_T}$  for forward-rapidity region, when no  $(p_T, \phi)$  acceptance restrictions have been used. It is evident that the qualitative structure of the energy dependence of  $\Phi_{p_T}$  is very similar also when using complete azimuthal angle acceptance. The  $\Phi_{p_T}$  values have been also calculated using forward-rapidity (anti-)protons only - also without  $(p_T, \phi)$  acceptance restrictions (solid lines in Fig. 4). Again, (anti-)protons follow the behavior observed in Fig. 2, thus indicating that the limited  $(p_T, \phi)$  acceptance indeed does not influence the observed effects significantly. In the studied forward-rapidity region (with  $0.005 < p_T < 1.5$  GeV/c cut) the total multiplicity of final state protons is similar for all five energies and varies between 42.4 and 47.6. Additionally, the  $\Phi_{p_T}$  values have been evaluated for the so-called ‘ $4\pi$ ’ acceptance which means that only transverse momentum cut ( $0.005 < p_T < 1.5$  GeV/c) has been used in the analysis (dotted lines in Fig. 4). However, in this ‘‘complete’’ kinematic acceptance the observed effect of interest seems to disappear. Instead, very small but negative  $\Phi_{p_T}$  values are obtained for lower SPS energies.

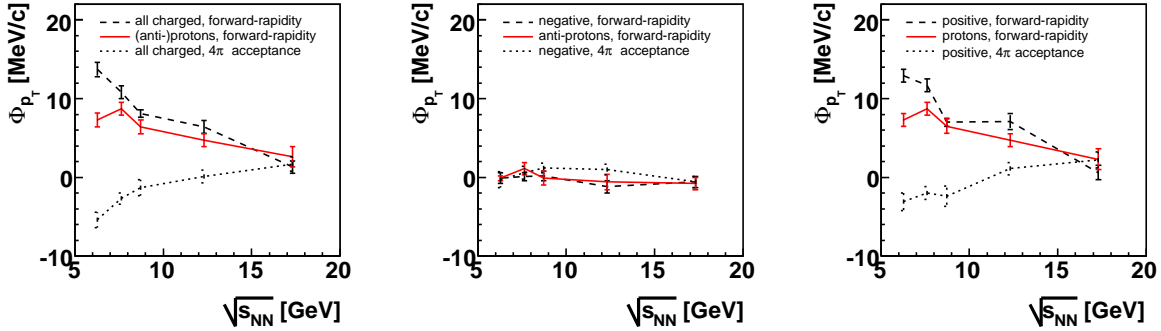


Figure 4: (Color online)  $\Phi_{p_T}$  versus energy calculated from the UrQMD model without  $(p_T - \phi)$  acceptance restrictions (applied by the NA49). Pion mass has been assumed for all produced particles. The dashed and solid lines correspond to forward-rapidity region ( $1.1 < y_\pi^* < 2.6$ ), and the dotted lines to ‘ $4\pi$ ’ acceptance. The panels represent: all charged, negatively charged and positively charged particles, respectively. Forward-rapidity (anti-)protons only are represented by solid lines.

So far, one has learned that the effect of increased transverse momentum fluctuations arises probably from protons only. Now, one can try to establish whether those are newly produced protons, spectators or participants. It has been shown in [4] that for lower SPS energies the NA49 acceptance for  $p_T$  fluctuations analysis extends to the beam spectator domain. Therefore a sample of particles used in the analysis can be contaminated by beam particles. Thus one can speculate that the increase of  $\Phi_{p_T}$  values may be somehow attributed to the presence of beam protons. Then, the measured correlation should be even stronger for the detector with complete (‘ $4\pi$ ’) acceptance because some of the beam particles - spectators or elastically rescattered protons - might hit into the midrapidity region or even into the backward hemisphere. Moreover, also participating neutrons (as neutral particles are not registered in the detector) should increase the total  $\Phi_{p_T}$  value. This hypothesis can be easily tested by use of the UrQMD events. The results of these calculations are presented in Fig. 5, where  $\Phi_{p_T}$  is calculated for ‘ $4\pi$ ’ acceptance ( $0.005 < p_T < 1.5$  GeV/c) for protons only (left) and for protons and neutrons (middle). The total multiplicity of protons is very similar for all five energies and varies between 167.1 and 169.9, whereas the total multiplicity of a mixture of protons with neutrons varies

between 358.9 and 366.1. The very strong fluctuations observed for protons only ( $\Phi_{p_T}$  at the level of 130 MeV/c) are exactly two times enlarged when neutrons are included. However, the  $\Phi_{p_T}$  values for several selections of newly produced particles such as pions or antiprotons remain very small even for ‘ $4\pi$ ’ acceptance (Fig. 5 - right), although the total multiplicity of all pions is much higher than the multiplicity of protons and neutrons together and strongly depends on the energy. This result seems to indicate that the dominant effect originate not from the newly produced particles but from beam/target nucleons.

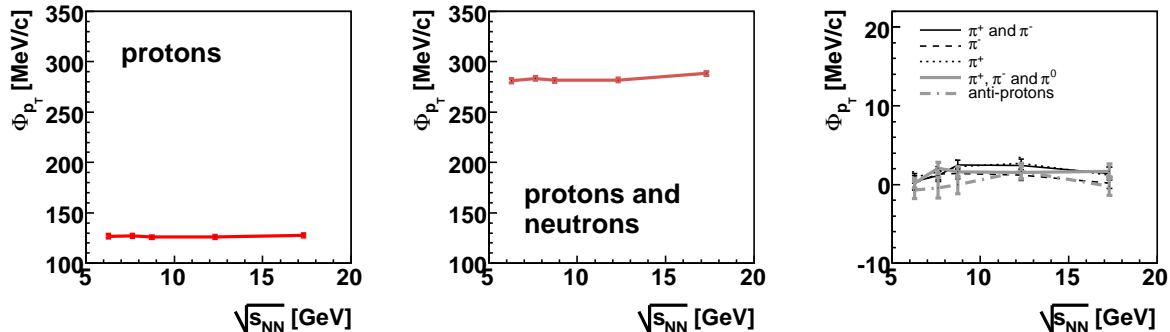


Figure 5: (Color online)  $\Phi_{p_T}$  versus energy calculated from the UrQMD model for ‘ $4\pi$ ’ acceptance ( $0.005 < p_T < 1.5$  GeV/c) for protons only (left), protons and neutrons (middle), and different selections of newly produced particles (right).

## 7 Correlation between the spectator and production regions

Within the NA49 acceptance (forward rapidity) the possible contamination from beam particles is the highest for 20A GeV interactions and therefore a test was carried out to check how the  $\Phi_{p_T}$  measure behaves when beam particles region is rejected. The NA49 results for 20A GeV Pb+Pb collisions are presented in Fig. 6, where the  $\Phi_{p_T}$  measure was evaluated as a function of an upper  $y_p^*$  cut ( $y_p^*$  is the particle rapidity calculated in the center-of-mass reference system assuming proton mass). In Fig. 6 the preliminary NA49 data are compared to predictions of the UrQMD model with the same acceptance restrictions. It is observed - both in the data and in the UrQMD model - that  $\Phi_{p_T}$  decreases when the number of rejected “beam particles” increases.

It has been also observed that although  $\Phi_{p_T}$  values measured with exclusion of the beam spectator region are low, the  $\Phi_{p_T}$  values obtained for “spectator only” region are also rather low, whereas the whole magnitude of  $p_T$  fluctuations can be reproduced only by using the whole rapidity interval. It suggests that the source of fluctuations is not concentrated at very forward rapidities only (beam spectator domain) but there might be a strong correlation between particles from beam spectator domain and particles at lower rapidities (even in the production region). The above effect has been observed both in the NA49 data and in the UrQMD events.

Figure 7 presents  $\Phi_{p_T}$  obtained for ‘ $4\pi$ ’ protons for the UrQMD 20A GeV interactions. The full points represent the increasing acceptance around the midrapidity region. The open points correspond to the increasing “gap” around midrapidity and thus selection of particles closer to beam/target spectator regions. Indeed, it can be observed that



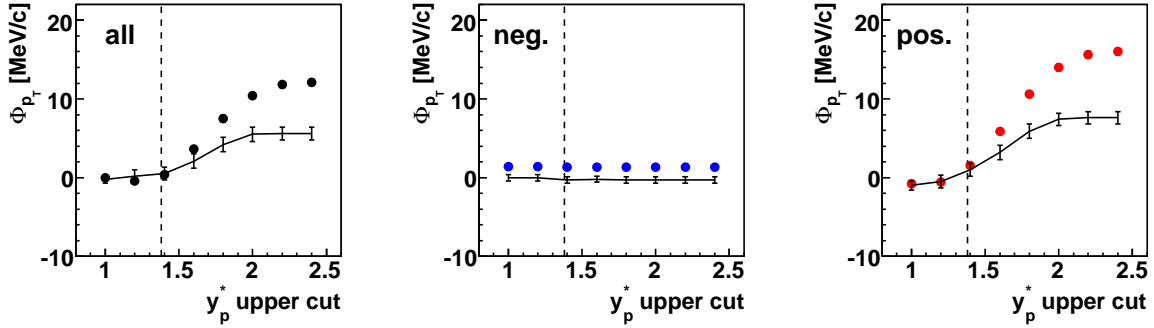


Figure 6: (Color online) The NA49 and UrQMD results on  $\Phi_{p_T}$  as a function of an upper  $y_p^*$  cut, obtained for 20A GeV interactions. Points represent the NA49 data with kinematic and acceptance restrictions as described in [4] and Sec. 3 (without  $y_p^*$  cut). Solid lines correspond to the UrQMD model with the acceptance restrictions the same as for the NA49 data. The NA49 data points are *not* corrected for limited two-track resolution. The panels represent: all charged, negatively charged, positively charged particles, respectively. For 20A GeV interactions the beam rapidity expressed in the center-of-mass reference system  $y_{beam}^* = 1.88$ . Note: the values and their errors are correlated. The dashed lines indicate the  $y_p^*$  cut finally used in the analysis of the NA49 20A GeV data. Figure taken from [4].

the maximal magnitude of  $\Phi_{p_T}$  (about 130 MeV/c) is obtained for a complete rapidity acceptance only, whereas  $\Phi_{p_T}$  values either in the spectator domain or in the midrapidity region are low.

## 8 The origin of correlation: event-by-event impact parameter fluctuations

The natural explanation of the effect described above consists in event-by-event impact parameter fluctuations or - more precisely - in correlation between the number of protons (nucleons) in the forward hemisphere and the number of protons (nucleons) in the production region. For more central events the number of forward-rapidity protons is smaller, and consequently, the number of protons in the production region is higher. The situation is opposite for less central collisions. The existence of those different event classes results in the increased  $\Phi_{p_T}$  values for positively charged particles.

A test of the hypothesis of the correlation between protons in different rapidity windows can be found in Fig. 8. Two kinds of the UrQMD particle samples: protons only and a mixture of protons and neutrons were used to obtain the  $\Phi_{p_T}$  dependence on the fraction of the total inelastic cross section of nucleus+nucleus collisions ( $\sigma/\sigma_{tot}$ ). The UrQMD calculations correspond to ‘4 $\pi$ ’ acceptance in both 20A and 158A GeV Pb+Pb interactions. The UrQMD results show a significant reduction of  $\Phi_{p_T}$  values when the centrality is restricted. The original  $\Phi_{p_T}$  value for protons only at the level of 130 MeV/c (for 7.2% most central interactions at 20A GeV) is reduced to the value consistent with zero when the centrality is restricted to 1% most central Pb+Pb interactions.

The similar effect was also observed within the NA49 acceptance region. Figure 9 presents the  $\Phi_{p_T}$  values - for 20A GeV interactions - plotted as a function of the fraction of the total inelastic cross section ( $\sigma/\sigma_{tot}$ ). The preliminary NA49 data were compared to the predictions of the UrQMD model with the same kinematic restrictions. Both the NA49 data (points) and the UrQMD events (lines) show a significant reduction of  $\Phi_{p_T}$

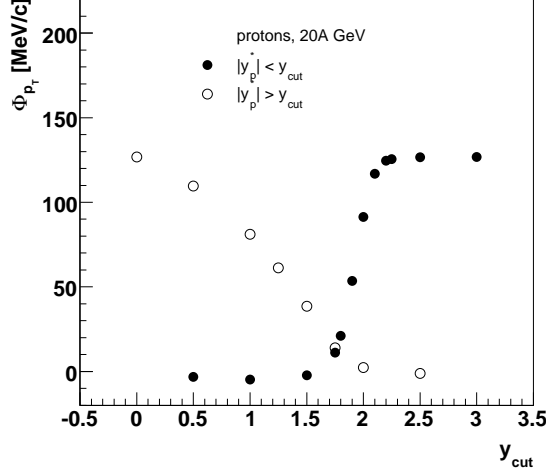


Figure 7:  $\Phi_{p_T}$  obtained for ‘ $4\pi$ ’ protons for the UrQMD 7.2% most central 20A GeV interactions. The full points represent the increasing acceptance around the midrapidity region. The open points represent the increasing ”gap” around midrapidity and selection of particles closer to beam/target spectator regions. For 20A GeV interactions the beam rapidity expressed in the center-of-mass reference system  $y_{beam}^* = 1.88$ . Note: the values and their errors are correlated.

values when the centrality is restricted to more central events.

The effect observed in Fig. 8 encourages us to study minimum bias interactions where impact parameter fluctuations from event to event should be maximal. The  $\Phi_{p_T}$  values, obtained for minimum bias 20A GeV UrQMD events (30k events), are demonstrated in Table 1. Results are shown for several particle selections at ‘ $4\pi$ ’ acceptance. Transverse momentum fluctuations for newly produced particles (pions) are consistent with zero, whereas for protons and for a sample of protons and neutrons - as it could be expected - exhibit extremely high  $\Phi_{p_T}$  values. Relatively high  $\Phi_{p_T}$  value can be also obtained when protons are combined with positively charged kaons and pions, whereas in the case of central data (Fig. 4) at ‘ $4\pi$ ’ acceptance, the presence of pions and kaons in a sample turned out to be sufficient to wash out the correlation originating from protons.

	$\Phi_{p_T}$ [MeV/c]	$\langle N \rangle$	$\sigma_N$
$p$	$1506 \pm 5.0$	167.1	6.2
$p$ and $n$	$2230.9 \pm 7.1$	402.5	16.3
$\pi^+$ and $\pi^-$	$-0.3 \pm 1.4$	157.5	171.8
$\pi^-$	$2.2 \pm 1.5$	83.5	90.7
$\pi^+$	$-1.2 \pm 1.4$	74.1	81.3
$\pi^+, \pi^-, p, \bar{p}, K^+, K^-$	$1106.7 \pm 4.7$	335.8	187.1
$\pi^-, \bar{p}, K^-$	$2.7 \pm 1.5$	86.1	93.8
$\pi^+, p, K^+$	$1290.6 \pm 4.1$	249.6	93.3

Table 1:  $\Phi_{p_T}$  values, mean multiplicities, and their dispersions ( $\sigma_N = \sqrt{\langle N^2 \rangle - \langle N \rangle^2}$ ) obtained for minimum bias 20A GeV UrQMD events (30k events). Results are shown for several particle combinations at ‘ $4\pi$ ’ acceptance.

Figures 7 and 8 together with the corresponding figures within the limited NA49 acceptance (Fig. 6 and Fig. 9) seem to confirm the hypothesis that the increased  $\Phi_{p_T}$  values can be indeed connected with event-by-event fluctuations of the number of protons in the forward hemisphere and the number of protons that are closer to the production

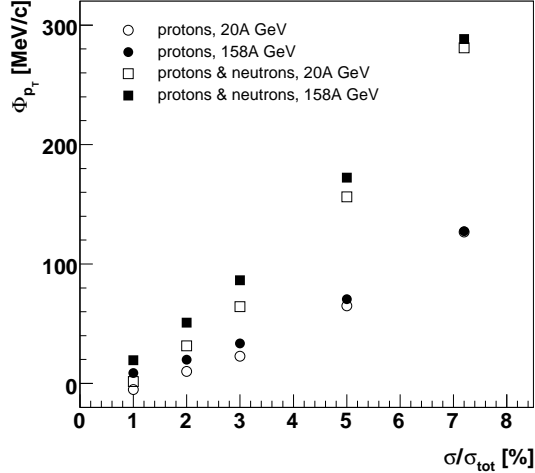


Figure 8:  $\Phi_{p_T}$  as a function of the fraction of the total inelastic cross section of nucleus+nucleus collisions ( $\sigma/\sigma_{tot}$ ). The results are obtained for ‘ $4\pi$ ’ protons or for a mixture of protons and neutrons for 20A GeV and 158A GeV UrQMD events. Note: the values and their errors are correlated.

region. There are at least two possible ways to eliminate this trivial source of correlations. The first - and the most natural one - consists in centrality restrictions, however it can significantly reduce the event statistics. The second one relies on applying an additional rapidity cut that would reject the beam spectator domain (see the vertical lines in Fig. 6).

The NA49 experiment chose the second (rejection) method and an additional  $y_p^*$  cut was applied for each energy, namely for each produced particle its  $y_p^*$  was required to be lower than  $y_{beam}^* - 0.5$ , where  $y_{beam}^*$  is the beam rapidity in the center-of-mass reference system. The final NA49 results on the  $\Phi_{p_T}$  fluctuation measure, as a function of energy, are shown in Fig. 10. Three panels represent all charged, negatively charged, and positively charged particles, respectively. The points correspond to the data (with statistical and systematic errors) and the lines to the predictions of the UrQMD model. When additional cut on  $y_p^*$  is applied, no significant energy dependence of  $\Phi_{p_T}$  measure can be observed for all three charge selections and  $\Phi_{p_T}$  values are consistent with the hypothesis of independent particle production (that is  $\Phi_{p_T} \approx 0$ ).

## 9 Final-state protons in the UrQMD model

The above analysis confirms that the preliminary NA49 results, i.e., the increased  $\Phi_{p_T}$  values at lower SPS energies were indeed due to protons only. The basic origin of this effect is the correlation between the number of protons (generally nucleons) in the forward hemisphere and the number of protons closer to the production region, caused by event-by-event impact parameter fluctuations. At the end of this analysis it is worthwhile to find out what is the origin of the final-state protons in the UrQMD model. In principle, it should be clarified what kind of protons are rejected by an additional cut on  $y_p^*$ , applied by the NA49 experiment.

Figure 11 shows the distributions of the number of collisions of final state protons, generated by the UrQMD model for the 7.2% most central Pb+Pb interactions at 20A GeV. Four panels correspond to different acceptance regions. The peaks at zero (upper

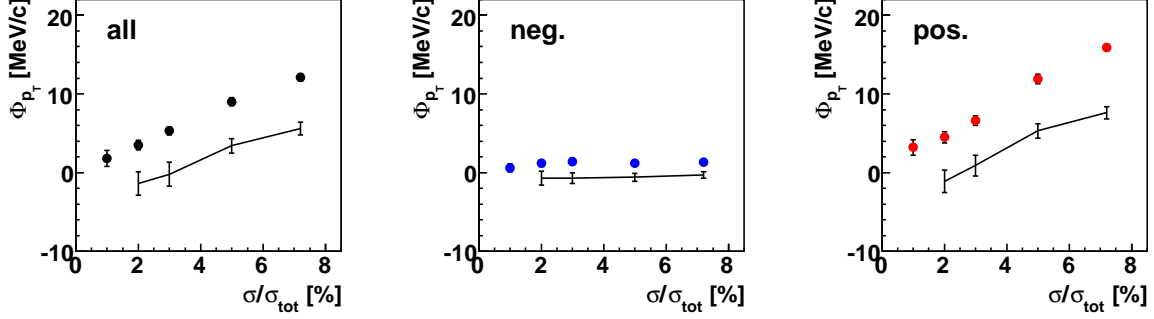


Figure 9: (Color online) The NA49 and UrQMD results on  $\Phi_{p_T}$  as a function of the fraction of the total inelastic cross section of nucleus+nucleus collisions ( $\sigma/\sigma_{tot}$ ) for 20A GeV Pb+Pb collisions. Points represent NA49 data with kinematic and acceptance cuts as described in Sec. 3 (without  $y_p^*$  cut). Solid lines correspond to the UrQMD model with the acceptance restrictions the same as for the NA49 data. The NA49 data points are *not* corrected for limited two-track resolution. The panels represent: all charged, negatively charged, and positively charged particles, respectively. Note: the values and their errors are correlated. Figure taken from [4].

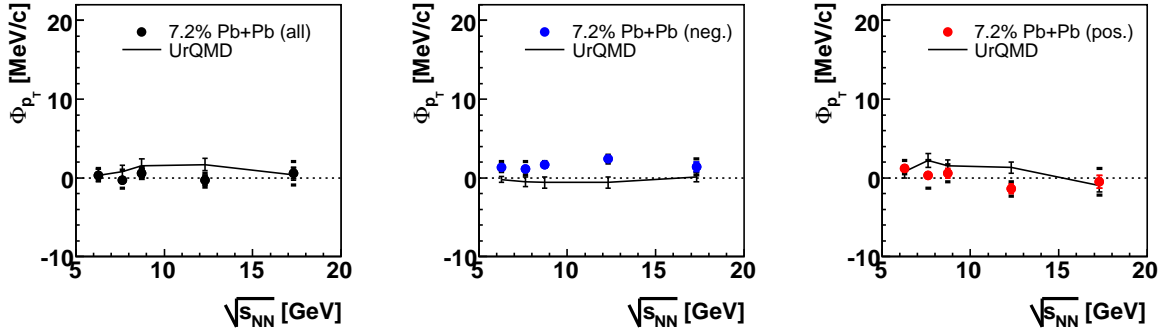


Figure 10: (Color online) The NA49 and UrQMD results on  $\Phi_{p_T}$  as a function of energy for the 7.2% most central Pb+Pb interactions for all charged particles (left) and for negatively charged (middle) and positively charged ones (right). The  $\Phi_{p_T}$  values are obtained with additional cut: only particles obeying  $y_p^* < y_{beam}^* - 0.5$ . NA49 data points are shown with statistical and systematic errors. The NA49 results are compared to the UrQMD predictions (solid lines) with the same acceptance restrictions. The NA49 data points taken from [4].

panels) represent real spectators, i.e., protons that do not experience any collision. Their fraction is obviously higher when one restricts rapidity acceptance to the regions closer to the rapidity of the beam (Fig. 11 upper, right). The mean number of collisions is generally smaller for the acceptance characteristic of the beam spectators (right panels). Fig. 11 (lower, left) shows protons in the acceptance selected by the NA49 experiment, whereas Fig. 11 (lower, right) - protons that were finally excluded from the NA49 acceptance by an additional cut on  $y_p^*$ . It is quite surprising that in the two lower panels there are no spectators ( $N_{coll} = 0$ ) at all. It would suggest that the effect of increased  $\Phi_{p_T}$  values was connected with participants only and that spectators did not play any important role. This is, however, true only inside the NA49 acceptance and it will be shown below (Table 2) that when the ‘ $4\pi$ ’ acceptance is considered, both real spectators and participants, i.e., elastically scattered protons (precisely, the correlation between multiplicities of those two) are responsible for the observed  $\Phi_{p_T}$  values.

During the collision process the projectile and target nucleons participate both in

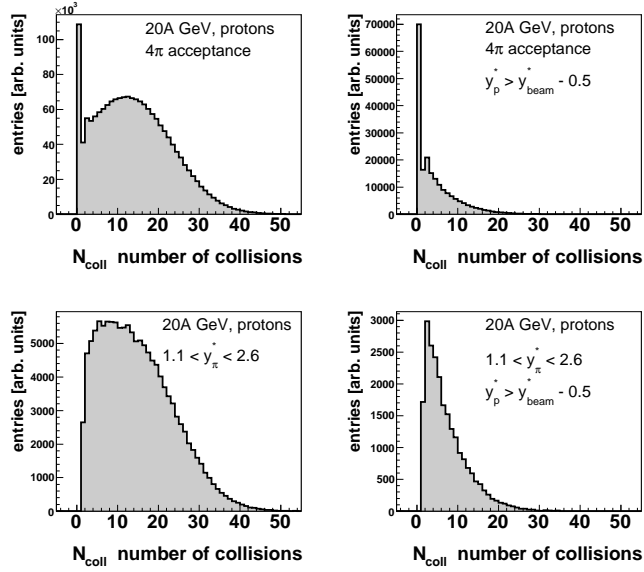


Figure 11: The distributions of the number of collisions of final-state protons generated by the UrQMD model for the 7.2% most central Pb+Pb interactions at 20A GeV. Different panels correspond to different acceptance regions.

elastic and inelastic interactions. In principle,  $\Delta$  resonances can be produced as an effect of inelastic collisions. Afterward,  $\Delta$ s decay into pions and nucleons. Technically - within the UrQMD model - for each final state particle one can attribute an integer number called the "ID of parent process", which describes the last process the particle was involved in. Therefore, it is easy to disentangle spectator protons from those originating from elastic or inelastic processes. Figure 12 presents the distributions of ID of parent process (last process the particle was involved in) obtained for the final-state protons generated in the UrQMD model for the 7.2% most central Pb+Pb interactions at 20A GeV. Different panels correspond to different acceptance regions - similarly to Fig. 11. Below, one can find a list of IDs that significantly contribute to the histogram.

The ID of parent process equal zero denotes real spectators ( $N_{coll} = 0$ ) but also elastically scattered protons (scattering with all barions and mesons is possible). For protons with ID of parent process equal zero the number of collisions ( $N_{coll}$ ) has a high peak at zero (real spectators) and a tail up to about 10-15, whereas the mean value of  $N_{coll}$  is about 0.5. All protons originating from decays (for example, from resonances) has ID of parent process equals 20. As we are considering central collisions (7.2%) the majority of protons come from decays with exception of very forward-rapidity regions where spectators begin to dominate (Fig. 12 upper, right). The ID of parent process equals 1 means protons generated in the reaction  $NN \rightarrow N\Delta^1$ , ID equals 14 means protons produced in inelastic interactions (without string excitation) such as:  $N^*N$ ,  $\Delta^*N$ ,  $\Delta N^*$ ,  $\Delta^*N^*$ , or  $N^*N^*$ . The parent history ID labeled as 30 denotes process  $\Delta N \rightarrow NN$ . And, finally, IDs equal 15 and 27 correspond to processes through 2 strings and process through 1 string, respectively.

Table 2 shows the  $\Phi_{pT}$  values for '4 $\pi$ ' protons obtained for UrQMD 7.2% most central Pb+Pb interactions at 20A GeV, where several choices of number of collisions ( $N_{coll}$ ) or ID of parent process have been applied. The  $\Phi_{pT}$  value obtained for spectators ( $N_{coll} = 0$ ) is low but it is low also when the spectators are rejected. The original magnitude of  $\Phi_{pT}$  (about 130 MeV/c) can be reproduced only when both spectators and "not spectators"

<sup>1</sup> $N \equiv N_{938}$  (nucleon),  $N^* \equiv N_{1440}, N_{1520}, N_{1535}, \dots$  (nucleon resonances),  $\Delta \equiv \Delta_{1232}, \Delta^* \equiv \Delta_{1600}, \Delta_{1620}, \Delta_{1700}, \dots$

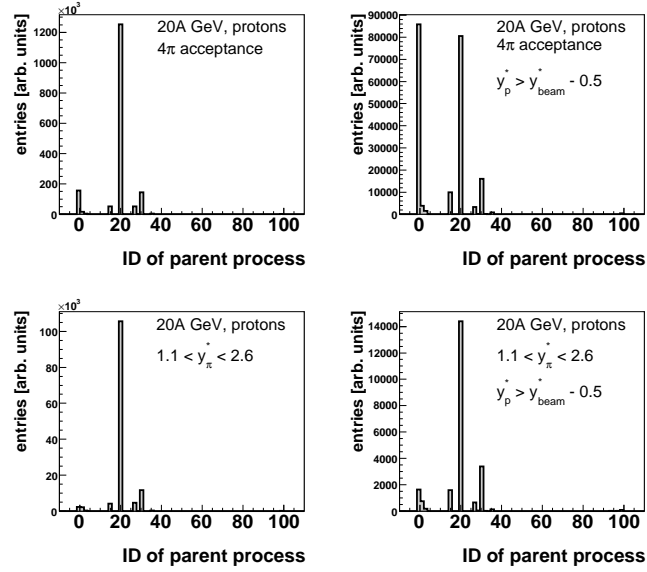


Figure 12: The distributions of ID of parent process (last process the particle was involved in) obtained for final-state protons generated by the UrQMD model for the 7.2% most central Pb+Pb interactions at 20A GeV. Different panels correspond to different acceptance regions.

are used in the analysis. It simply indicates that there should be some kind of correlation between spectators and “not spectators”. The same observation can be achieved for ID of parent process equal and not equal zero. The opposite situation takes place when protons originating from decays are considered. The  $\Phi_{p_T}$  value evaluated for protons coming from decays is rather low: however, if such protons are rejected from the analysis, - the  $\Phi_{p_T}$  does not decrease but even increases! It means that protons from decays (i.e. newly produced particles) do not generate the dominant correlation in the analysis. It is in agreement with intuitive predictions, because also newly produced particles such as pions, kaons, or antiprotons lead to  $\Phi_{p_T}$  value consistent with zero. Finally, it has been observed that not only protons from decays but also protons created in a list of inelastic processes (labeled as 1, 14, 15, 27, 30) result in a  $\Phi_{p_T}$  values consistent with zero. Therefore it can be concluded that the whole effect of the increased transverse momentum fluctuations comes from beam/target particles only (both real spectators and elastically scattered beam/target protons). Those particles can hit different rapidity windows - depending on the centrality of a given event. Consequently, the sample composed by a mixture of events with different impact parameters generates increased event-by-event  $p_T$  fluctuations. The impact parameter range in the 7.2% most central Pb+Pb interactions is wide enough to produce significantly increased  $\Phi_{p_T}$  values.

	$\Phi_{pT}$ [MeV/c]	$\langle N \rangle$	$\sigma_N$
rejection of protons with $N_{coll} = 0$ (spectators)	$35.5 \pm 1.4$	158.2	10.3
only protons with $N_{coll} = 0$ (spectators)	$4.5 \pm 0.2$	10.8	6.0
rejection of protons with ID of parent process = 0 (spectators and elastically scattered protons)	$16.3 \pm 1.4$	153.5	11.2
only protons with ID of parent process = 0 (spectators and elastically scattered protons)	$5.8 \pm 0.7$	15.6	7.9
rejection of protons with ID of parent process = 20 (protons from decays)	$156.7 \pm 1.6$	43.7	10.1
only protons with ID of parent process = 20 (protons from decays)	$12.6 \pm 1.2$	125.3	11.5
rejection of protons with ID of parent process = 1 ( $NN \rightarrow N\Delta$ )	$125.2 \pm 1.5$	167.4	9.2
only protons with ID of parent process = 1 ( $NN \rightarrow N\Delta$ )	$1.9 \pm 1.2$	1.7	1.3
rejection of protons with ID of parent process = 14 ( $N^*N, \Delta^*N, \Delta N^*, \Delta^*N^*$ or $N^*N^*$ )	$127.5 \pm 1.4$	166.3	9.2
only protons with ID of parent process = 14 ( $N^*N, \Delta^*N, \Delta N^*, \Delta^*N^*$ or $N^*N^*$ )	$1.8 \pm 1.6$	2.7	1.7
rejection of protons with ID of parent process = 15 (process through 2 strings)	$125.8 \pm 1.4$	166.5	9.2
only protons with ID of parent process = 15 (process through 2 strings)	$1.3 \pm 1.2$	2.5	1.6
rejection of protons with ID of parent process = 27 (process through 1 string)	$127.3 \pm 1.4$	163.9	9.2
only protons with ID of parent process = 27 (process through 1 string)	$0.8 \pm 1.0$	5.1	2.3
rejection of protons with ID of parent process = 30 ( $\Delta N \rightarrow NN$ )	$126.9 \pm 1.4$	155.0	9.1
only protons with ID of parent process = 30 ( $\Delta N \rightarrow NN$ )	$2.7 \pm 1.1$	14.0	4.3

Table 2:  $\Phi_{pT}$  values, mean multiplicities, and their dispersions ( $\sigma_N = \sqrt{\langle N^2 \rangle - \langle N \rangle^2}$ ) obtained for UrQMD 7.2% most central Pb+Pb interactions at 20A GeV. Results are shown for protons at ‘4 $\pi$ ’ acceptance with several choices of number of collisions ( $N_{coll}$ ) or ID of parent process (see the text for details).

## 10 Summary and Conclusions

It has been presented how event-by-event impact parameter fluctuations influence transverse momentum fluctuations. In principle, it has been explained that the preliminary NA49 results - showing significantly increased  $\Phi_{p_T}$  values at lower SPS energies - are connected with the trivial effects of impact parameter fluctuations. It suggests that a precise selection of very narrow centrality bins should be crucial not only for the analysis of multiplicity fluctuations [9] but also for transverse momentum fluctuations and probably for other kinematic characteristics.

It was predicted that either approaching the phase boundary of the QCD phase diagram or hadronization close to the critical point should lead to increased values of transverse momentum fluctuations. Therefore it is very important to distinguish between interesting physical effects and trivial ones as those connected with impact parameter fluctuations. Below, one can find several methods to eliminate the effects of event-by-event impact parameter fluctuations.

1. One can perform the analysis for all three charge selections (all charged, negatively charged, positively charged) and check whether the same structure (not necessarily the magnitude!) of  $\Phi_{p_T}$  versus energy or centrality (system size) appears for all possible charge selections (see the NA49 results in [3]).
2. If the previous method is not possible it is safer to restrict the analysis to negatively charged particles only, instead of all charged or positively charged ones.
3. The experiments with reliable particle identification can try to reject protons from the sample and measure  $\Phi_{p_T}$  for newly produced particles only (pions or a mixture of pions, kaons, etc.).
4. One can also probe the midrapidity region only (production domain) or at least one can check whether the selected acceptance does not extend to the beam/target spectator domain.
5. The best and the least controversial method relies on a drastic centrality restriction. However, due to insufficient statistics, this method cannot be applied by every experiment.

It has been already mentioned that due to the specific choice of the rapidity region (midrapidity only) the RHIC experiments are essentially free of the effects of impact parameter fluctuations, even though in most cases the results are obtained by use of all charged particles registered in the detectors. The same remark concerns also the CERES experiment at CERN SPS that measured transverse momentum fluctuations in 40A, 80A, and 158A GeV Pb+Au interactions by use of all charged particles - but produced in midrapidity region only [8]. In contrary, the acceptance of the NA49 experiment - selected for the analysis of transverse momentum fluctuations - extends to the beam spectator domain. However, the NA49 experiment performs the analysis by use of all three charge selections and therefore it was possible to separate and finally eliminate the trivial effects connected with the impact parameter fluctuations.



## Acknowledgments

I am indebted to the authors of the UrQMD model for the permission to use their code in my analysis. I am very grateful to Marek Gaździcki for his interesting comments and suggestions concerning this analysis. I also appreciate the editorial remarks from Ewa Skrzypczak and Staszek Mrówczyński. Finally I thank Jarek Grebieszko for the software support.

## References

- [1] M. Stephanov, K. Rajagopal, and E. V. Shuryak, *Event-by-event fluctuations in heavy ion collisions and the QCD critical point*, *Phys. Rev.* **D60**, 114028 (1999).
- [2] M. Gaździcki and St. Mrówczyński, *A method to study 'equilibration' in nucleus-nucleus collisions*, *Z. Phys.* **C54**, 127 (1992).
- [3] T. Anticic et al. (NA49 Collab.), *Transverse Momentum Fluctuations in Nuclear Collisions at 158 AGeV*, *Phys. Rev.* **C70**, 034902 (2004).
- [4] K. Grebieszko et al. (NA49 Collab.), *Event-by-event transverse momentum fluctuations in nuclear collisions at CERN SPS*, to be published in *PoS (CPOD07)* **022**, [[arXiv:0707.4608](#) [[nucl-ex](#)]].
- [5] S. A. Bass et al., *Microscopic Models for Ultrarelativistic Heavy Ion Collisions*, *Prog. Part. Nucl. Phys.* **41**, 225 (1998).
- [6] M. Bleicher et al., *Relativistic Hadron-Hadron Collisions in the Ultra-Relativistic Quantum Molecular Dynamics Model (UrQMD)*, *J. Phys.* **G25**, 1859 (1999).
- [7] M. Bleicher et al., *Can momentum correlations proof kinetic equilibration in heavy ion collisions at 160-A-GeV?*, *Phys. Lett.* **B435**, 9 (1998).
- [8] D. Adamova et al. (CERES Collaboration), *Event-by-event fluctuations of the mean transverse momentum in 40, 80, and 158 AGeV/c Pb-Au collisions*, *Nucl. Phys.* **A727**, 97 (2003).
- [9] C. Alt et al. (NA49 Collab.), *Centrality and system size dependence of multiplicity fluctuations in nuclear collisions at 158A GeV*, *Phys. Rev.* **C75**, 064904 (2007).